Supplemental Data

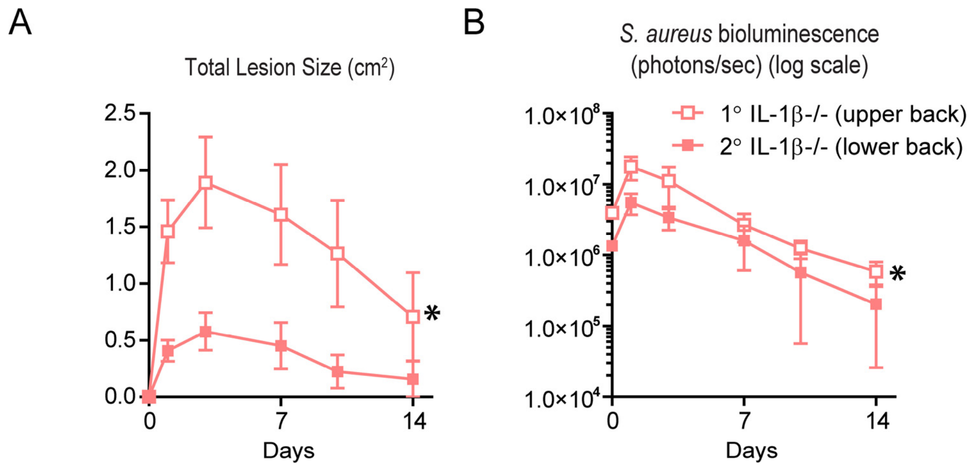

Supplemental Figure 1. Protection in IL-1$\beta^{-/-}$ mice is not limited to a specific skin location. The location of skin inoculation of the bacteria were reversed in which the 1° infection was performed in the upper back and the 2° infection performed on lower back (n=5/group). (A) Mean total lesion size (cm^2) ± SEM. (B) Mean total flux (photon/s) ± SEM. *P<0.05, as measured by two-way ANOVA.

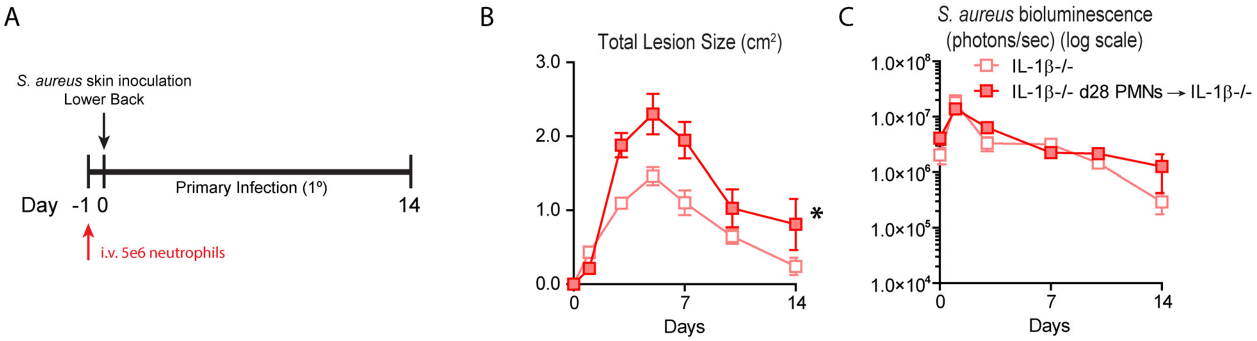

Supplemental Figure 2. Neutrophils from previously infected IL-1$\beta^{-/-}$ mice do not confer protection to naïve IL-1$\beta^{-/-}$ mice. (A) Timeline for transfer of neutrophils harvested from day 28 IL-1$\beta^{-/-}$ mice to naïve IL-1$\beta^{-/-}$ mice. (B) Mean total lesion size (cm^2) ± SEM. (C) Mean total flux (photon/s) ± SEM. *P <0.05, as measured by two-way ANOVA.

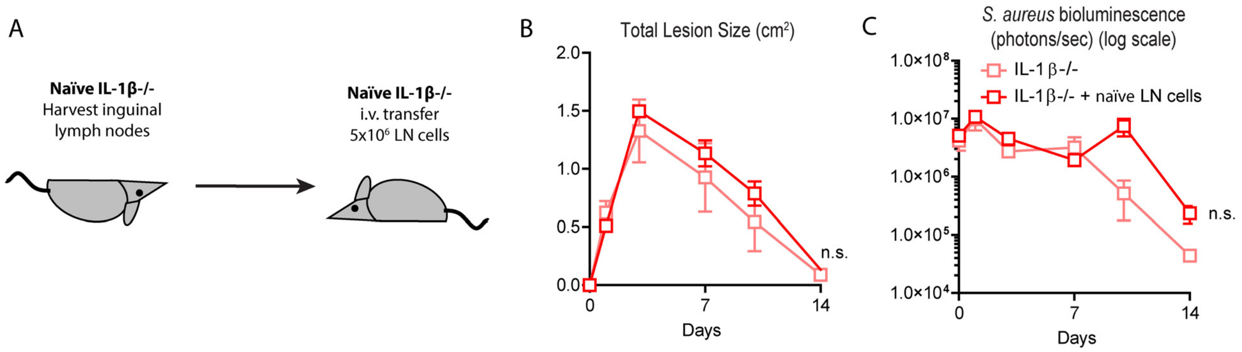

Supplemental Figure 3. Transfer of naïve lymph node cells from IL-1β$^{-/-}$ mice do not confer protection. (A) Timeline of harvesting and transferring of 5×10^6 lymph node cells from naïve IL-1β$^{-/-}$ mice into naïve IL-1β$^{-/-}$ recipients (n=5/group). (B) Mean total lesion size (cm^2) ± SEM. (C) Mean total flux (photon/s) ± SEM.

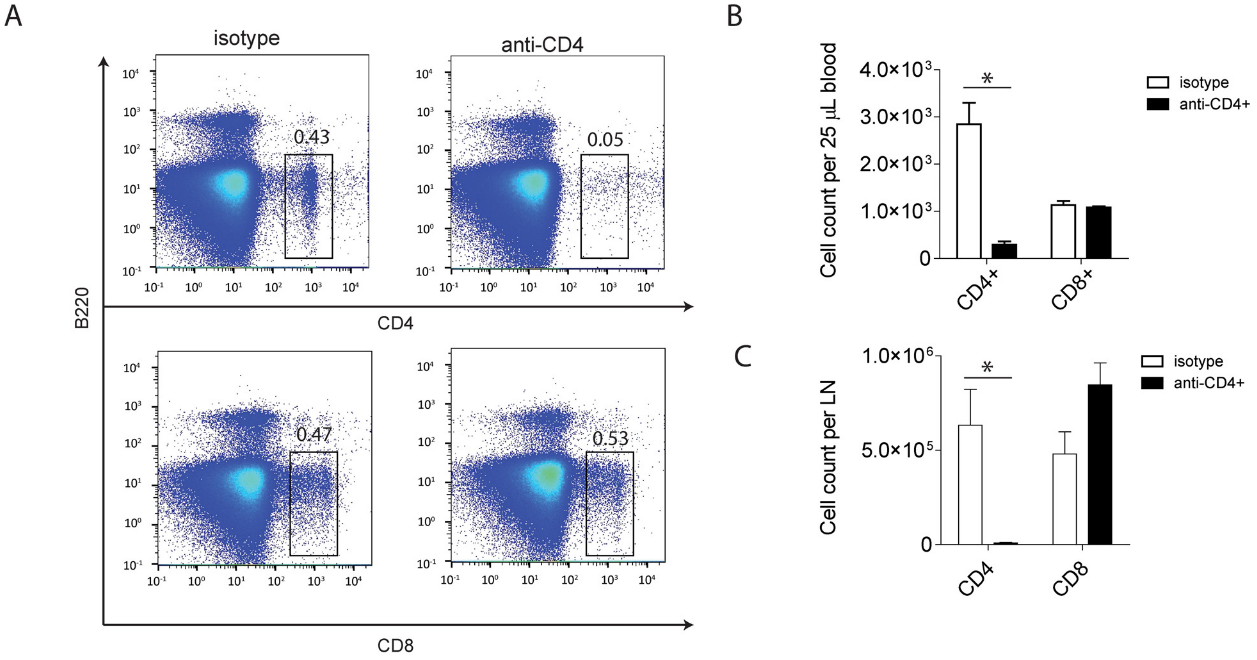

Supplemental Figure 4. Anti-CD4 antibody selectively depletes CD4$^+$ T cells. (A,B) Representative flow plots (A) and mean percentages of CD4$^+$ and CD8$^+$ T cells ± SEM in peripheral blood (B) and lymph nodes (LNs) (C) following isotype or anti-CD4 antibody treatment at the experimental endpoint (14 days after *S. aureus* skin inoculation). **P* <0.05, as measured by a two-tailed Student's t-test.

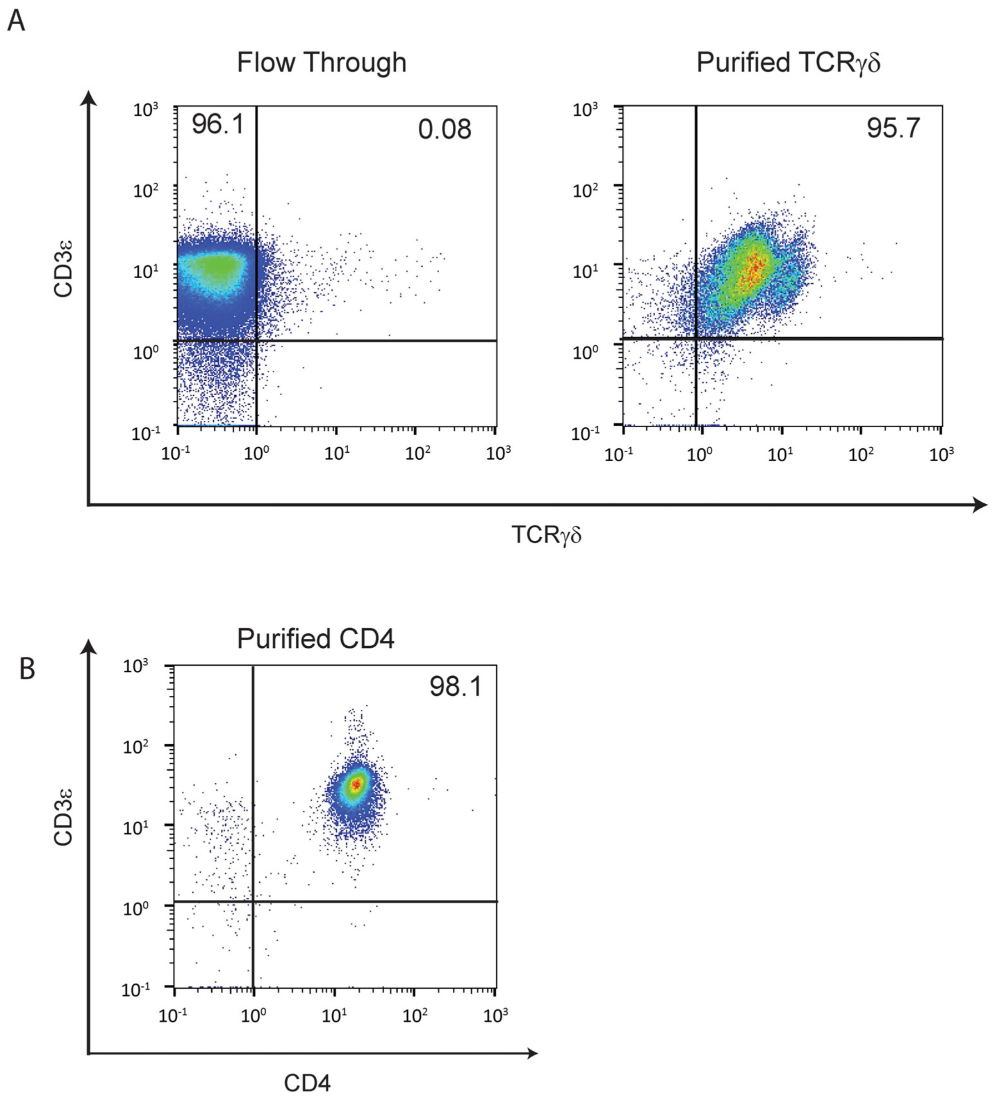

Supplemental Figure 5. Purification of γδ T cells from lymph nodes harvested on day 28 from previously infected IL-1$\beta^{-/-}$ mice. (A) Representative flow plots with percentages of TCRγδ+ cells in Flow Through or Purified TCRγδ populations prior to transfer into naïve IL-1$\beta^{-/-}$ mice. (B) Representative flow plots with percentages of CD4^{+} T cells prior to transfer into naïve IL-1$\beta^{-/-}$ mice.

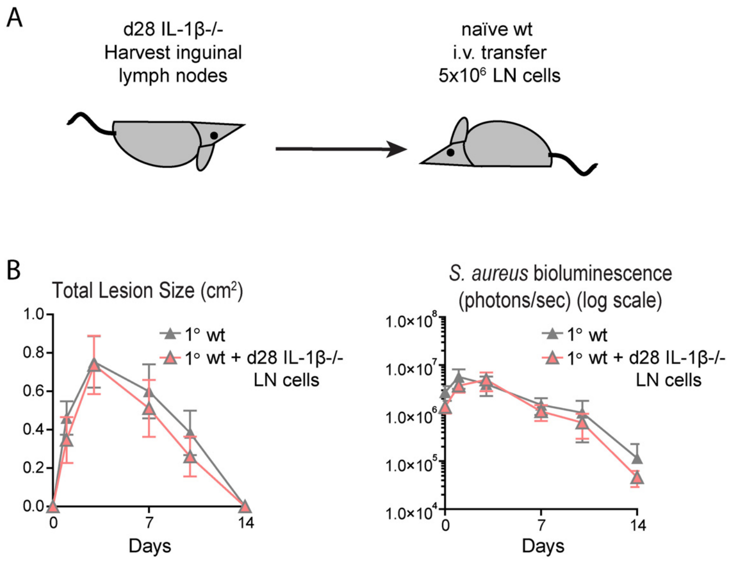

Supplemental Figure 6. Transfer of lymph node cells from day 28 IL-1β-/- mice does not provide protection to naïve wt mice. (A) Timeline of harvesting and transferring of $5x10^6$ lymph node cells from d28 IL-1β—/— mice into naïve wt recipients (n=5/group) (B) Mean total lesion size (cm^2) ± SEM. (C) Mean total flux (photon/s) ± SEM.

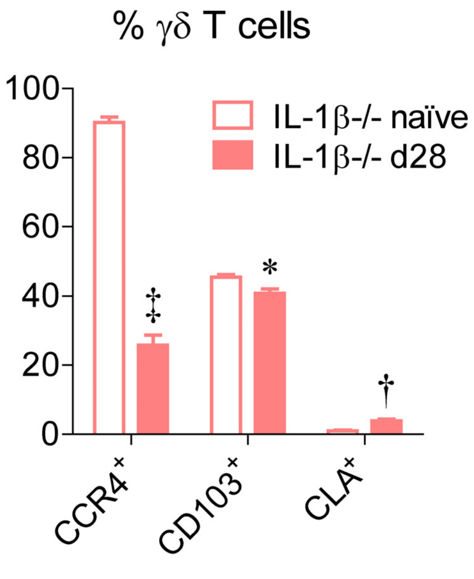

Supplemental Figure 7. Expression of homing and adhesion molecules on γδ T cells. γδ T cells were isolated from naïve and day 28 IL-1β—/— mice (n=5/group) and were assessed for CCR4, CD103 and CLA expression by FACS. Mean percentages of $CCR4^+$, $CD103^+$ and CLA^+ γδ T cells ± SEM. **P* <0.05, †*P* <0.01, ‡*P* <0.001 as measured by a Student's t-test.

Gene	**Mouse**	**Spearman TRGV5/6**	***P* value**	**Spearman TRDV4**	***P* value**
SKINT1	IL-1β-/-	-0.19	3.99×10^{-01}	-0.12	$5.91\ 10^{-01}$
SKINT3	IL-1β-/-	0.05	8.36×10^{-01}	-0.06	$7.82\ 10^{-01}$
SKINT9	IL-1β-/-	-0.18	3.85×10^{-01}	-0.20	$3.74\ 10^{-01}$
BTNL2	IL-1β-/-	0.62	2.13×10^{-03}	0.72	$1.66\ 10^{-04}$

Supplemental Figure 8. Spearman correlations of reads mapping to butyrophilin family members with reads mapping to the CDR3-encoding nt sequences of the dominant *TRG*-encoded and *TRD*-encoded CDR3 aa sequences identified in Figure 8B in lymph nodes from IL-1β—/— mice. Correlations were assessed between the following butyrophilin family members (*BTN1A1*, *BTNL1*, *BTNL2*, *BTNL4*, *BTNL6*, *BTNL9*, *BTNL10* and *ERG3*) including the *SKINT* family members (*SKINT1-SKINT11*) and only *BTLN2* had a statistically significant correlation (shown in red). For comparison, the correlations with *SKINT1*, *SKINT3* and *SKINT9* are shown because these butyrophilin family members have been previously implicated as ligands or co-stimulatory molecules for DETCs, which have the same CDR3 aa sequences as the expanded *TRG*-encoded and *TRD*-encoded CDR3 aa sequence identified in Figure 8B.

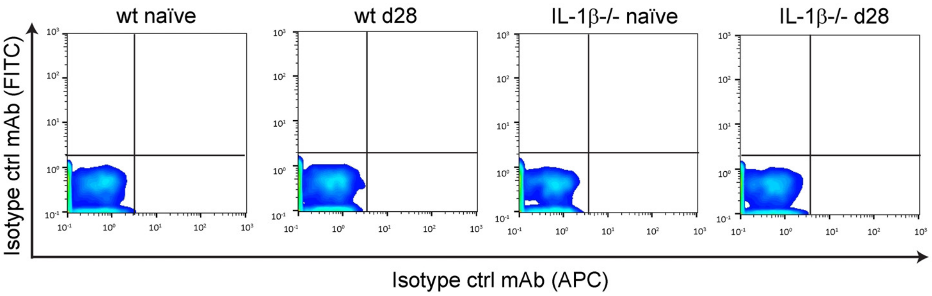

Supplemental Figure 9. Representative FACS plots for the isotype control mAbs corresponding to the intracellular staining for anti-IL-17A, anti-IL-22, anti-TNF and anti-IFNγ mAbs used in Figure 7A.